AMSI VACATION RESEARCH SCHOLARSHIPS 2018-2019

Developing a Within-Host Model for *Plasmodium vivax* in an Endemic Setting

Somya Mehra
Supervised by Dr Jennifer Flegg and Prof James McCaw
University of Melbourne

Vacation Research Scholarships are funded jointly by the Department of Education and Training and the Australian Mathematical Sciences Institute.

AMSI AUSTRALIAN MATHEMATICAL SCIENCES INSTITUTE

Australian Government
Department of Education and Training

Abstract

Malaria is an infectious disease with an immense global health burden. *Plasmodium vivax* is the most geographically-widespread species of malaria. Relapsing infections are a critical feature of the epidemiology of *Plasmodium vivax*, augmenting the difficulty of treatment, elimination and control. Relapses also have important consequences for the acquisition of immunity, allowing immunity to be gained relatively rapidly, even in areas of low transmission. Previous efforts to model blood-stage immunity to vivax malaria in transmission settings have been limited. In this project, a stochastic within-host model for blood-stage immunity to vivax malaria has been developed. A moment generating function for blood-stage immunity has been derived in a general framework, allowing parameters of epidemiological interest to be extracted for a broad range of biologically-relevant scenarios.

Introduction

The global malaria burden is immense, with an estimated 216 million cases and 445,000 deaths globally in 2016 (WHO, 2017). The primary pathogens responsible for human malaria are *Plasmodium falciparum* and *Plasmodium vivax*. As the most geographically widespread species of human malaria, *Plasmodium vivax* contributes to a significant proportion of the malaria burden beyond sub-Saharan Africa, causing 64% of malaria cases in the Americas, 30% in South East Asia and 50% in the Eastern Meditteranean (WHO, 2017). Historically neglected as a benign form of malaria, *Plasmodium vivax* has received far less scientific attention than *Plasmodium falciparum* However, associations between *Plasmodium vivax* and severe disease have become apparent in recent years (Naing, 2014). Control and elimination strategies designed for *Plasmodium falciparum* are not always applicable to *Plasmodium vivax* (Howes *et al*, 2016) Relapsing infections, in particular, exacerbate the difficulty of treating, eliminating and controlling *Plasmodium vivax*.

Parasite Lifecycle

Like all species of malaria, the transmission of *Plasmodium vivax* is mediated by *Anopheles* mosquito vectors. During a blood meal, an infected mosquito vector will inject sporozoites into the bloodstream of a human host. Sporozoites will then travel to the liver and invade individual liver cells (Mueller *et al*, 2013). Within a liver cell, a sporozoite has two possible fates: it may develop into either an active liver schizont, or a dormant hypnozoite. An active liver schizont will rupture within a period of 5 to 8 days, giving rise to a *primary infection* (Mueller *et al*, 2013). A hypnozoite, in contrast, will remain dormant for an indeterminate period but may cause a *relapse* upon activation (Mueller *et al*, 2013). Each infected mosquito bite thus gives rise to a single primary infection, and a variable number of relapses that can be spread apart quite far in time. Both primary infections and relapses involve the circulation of blood-stage parasites in the host bloodstream.

Immunity

Immunity is gained through cumulative exposure to parasite antigens. Immunity, however, also decays in the absence of exposure; regular antigenic exposure is required to maintain high levels of immunity (Mueller *et al*, 2013). There is an emerging consensus that acquired immunity to *Plasmodium vivax* is largely targeted

at blood-stage parasites, and is thus contingent on primary infections and relapses (Mueller *et al*, 2013). Relapsing infections thus have important consequences for the acquisition of immunity, allowing immunity to be gained rapidly even with low levels of mosquito transmission (Mueller *et al*, 2013). *Blood-stage immunity* can be thought to modulate both parasite levels and the risk of clinical symptoms such as fever during blood-stage infection.

Modelling Immunity to *Plasmodium vivax*

Efforts to model blood-stage immunity to *Plasmodium vivax* in transmission settings have been limited. Within-host models simulating the interactions of parasite and human cells have been developed to understand mechanisms of blood-stage immunity to *Plasmodium vivax* (McQueen and McKenzie, 2008; Kerlin and Gatton, 2015). Transmission blocking immunity, which reduces the probability of mosquitoes picking up parasites from infected humans, has been examined in transmission settings (De Zoysa *et al*, 1991). However, we are unaware of an existing within-host model that considers the gain of blood-stage immunity over a lifetime in an endemic region. In this project, we have developed a stochastic within-host model of blood-stage immunity to *Plasmodium vivax* for an individual in an arbitrary transmission setting. Our model of immunity is governed by two complementary dynamics: immunity is boosted with every infection experienced, but is also subject to decay over time.

Modelling Relapses as an Infinite Server Queue

During 2018, working with my supervisors on a voluntary basis, I developed a within-host model for the cumulative number of relapses experienced by an individual. The premise of the model is to conceptualise relapses as a $M_t^X/G/\infty$ queue (Eick, Massey and Whitt, 1991; Holman, Chaudhry and Kashyap, 1982). Mosquito bites, which constitute the arrival process, are modelled as a compound, non-homogenous Poisson process, allowing for variations in the bite rate and the number of hypnozoites conferred with each bite. Hypnozoites remain in the queue whilst dormant, and leave the queue upon activation. Service times, which represent hypnozoite dormancies, are informed by an underlying model of hypnozoite activation adapted from White *et al* (2014). By studying the departure process of our queue, we can track the number of relapses experienced by an individual over time. The observation that the departure process for the $M_t^X/G/\infty$ queue is a filtered Poisson process (Holman, Chaudhry and Kashyap, 1982) has underpinned the analysis of our model of blood-stage immunity.

Analysis

We develop a within-host model for blood-stage immunity to *Plasmodium vivax* progressively, beginning with a model for mosquito bites. We devise a model for the activation of a single hypnozoite, and then extend our model to consider relapses arising from a single bite. We then model the immunity gained from a single bite conferring a known number of hypnozoites, before extending our analysis to immunity gained from a stream of mosquito bites, each of which confers a variable number of hypnozoites.

Mosquito Bites

We model mosquito bites as a compound nonhomogeneous Poisson process. We assume bites occur at a time-dependent rate $\lambda(t)$, allowing us to account for seasonality and environmental changes. The mean number of bites in the interval $[0, t)$ is

$$m(t) = \int_0^t \lambda(\tau) d\tau$$

We also allow for variation in the number of hypnozoites conferred by each bite. Similarly to White *et al* (2014), we assume that the number of hypnozoites N conferred by each bite is geometrically-distributed with mean ν. Hence, the probability of a bite containing n hypnozoites is

$$\Pr(N = n) = g_n = \frac{1}{\nu + 1}\left(\frac{\nu}{\nu + 1}\right)^n$$

We treat the arrival processes of bites conferring different numbers of hypnozoites to be statistically independent. Bites conferring exactly n hypnozoites are therefore modelled to follow a Poisson distribution with rate parameter $g_n\lambda(t)$ given by the product of the overall bite rate $\lambda(t)$ and the probability g_n of a bite containing n hypnozoites.

Hypnozoite Activation

We begin by modelling the activation of a single hypnozoite. We adapt the model of hypnozoite activation developed by White *et al* (2014) in which hypnozoites undergo a latency phase before they are susceptible to activation. Similarly to White *et al* (2014), we model this latency phase as an Erlang distribution with rate parameter δ and k compartments, as shown in Figure 1. The variance in the length of the latency phase can be decreased by increasing the number of compartments k. The expected length of the latency phase is k/δ. During the latency phase, we assume a constant death rate μ for each hypnozoite, either due to the death of the hypnozoite itself or the host liver cell (White *et al*, 2014). We model activation to occur at a constant rate α once a hypnozoite reaches the final compartment of the latency phase (White *et al*, 2014). In contrast to White's model, we allow hypnozoites established through the same mosquito bite to proceed through the compartments of the latency phase independently. This overcomes an issue in White's model, whereby progress through the latency phase was enforced to be in 'lock step' for hypnozoites from the same mosquito bite.

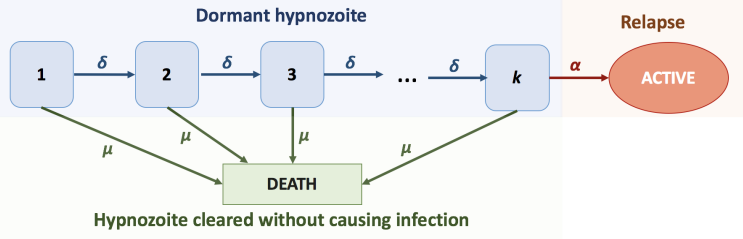

Figure 1: Schematic for model of activation for a single hypnozoite

Let $p_{\mathrm{m}}(t)$ be the probability that a hypnozoite is in compartment m of the latency phase at time t; $p_{\mathrm{active}}(t)$ be the probability that a hypnozoite has relapsed into a blood infection at time t and $p_{\mathrm{death}}(t)$ be the probability that the hypnozoite death has occurred by time t. Then we obtain the set of differential equations describing the state of a single hypnozoite time t after inoculation

$$\begin{aligned}
\frac{dp_1}{dt} &= -(\mu+\delta)p_1(t) && (1)\\
\frac{dp_m}{dt} &= -(\mu+\delta)p_m(t) + \delta p_{m-1}(t),\ m \in [2, k-1] && (2)\\
\frac{dp_k}{dt} &= -(\alpha+\mu)p_k(t) + \delta p_{k-1}(t) && (3)\\
\frac{dp_{\mathrm{active}}}{dt} &= \alpha p_k(t) && (4)\\
\frac{dp_{\mathrm{death}}}{dt} &= \mu \sum_{i=1}^{k} p_i(t) + \mu p_{\mathrm{active}}(t) && (5)
\end{aligned}$$

When a mosquito bite occurs, we assume each hypnozoite starts in the first compartment of the latency phase, yielding initial conditions

$$p_1(0) = 1, p_c(0) = p_{\mathrm{active}}(0) = p_{\mathrm{death}}(0) = 0 \text{ for } c > 1 \tag{6}$$

We solve system (1)-(5), with initial conditions (6) iteratively using integration by parts

$$\begin{aligned}
p_m(t) &= \frac{(\delta t)^{m-1}}{(m-1)!} e^{-(\mu+\delta)t} \text{ for } m \in [1, k-1]\\
p_k(t) &= e^{-(\mu+\alpha)t} \frac{\delta^{k-1}}{(k-2)!} \int_0^t t'^{k-2} e^{(\alpha-\delta)t'} dt'\\
p_{\mathrm{active}}(t) &= \frac{\alpha\delta^{k-1}}{(k-2)!} \int_0^t e^{-(\mu+\alpha)t'} \int_0^{t'} t''^{k-2} e^{(\alpha-\delta)t''} dt'' dt'\\
p_{\mathrm{death}}(t) &= 1 - \sum_{i=1}^{k} p_i(t) - p_{\mathrm{active}}(t)
\end{aligned} \tag{7}$$

Figure 2 shows the probability of activation for a single hypnozoite with a long latency period, parameterised using values taken from White *et al* (2014).

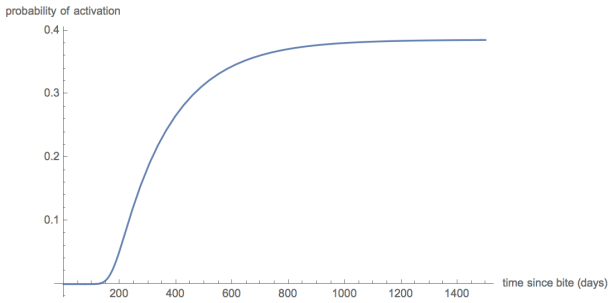

Figure 2: Probability of activation for a single hypnozoite with $\delta = 0.2$ day^{-1}, $k = 36$, $\alpha = 1/325$ day^{-1}, $\mu = 1/442$ day^{-1}. Parameters have been taken from White *et al* (2014).

Infections for a Single Bite

Consider a single bite conferring n hypnozoites. Define $J_n(t)$ and $I_n(t)$ to be random variables describing the number of relapses and infections time t after the bite. Since the incubation period of a primary infection is expected to be substantially shorter than the latency period for a relapse (White and Imwong, 2012), we assume that a primary infection is developed immediately after the bite. Hence

$$I_n(t) = J_n(t) + 1$$

Suppose that hypnozoite dormancies are independent and identically-distributed (i.i.d.) with distribution

$$B(t) = p_{\text{active}}(t) = \text{probability hypnozoite has activated by time } t$$

given by our within-host model for hypnozoite activation (7). We have replaced $p_{\text{active}}(t)$ with $B(t)$ for notational convenience. Then it follows that

$$J_n(t) \sim \text{Binomial}(B(t), n)$$

Since $I_n(t)$ is a linear combination of a binomial random variable $J_n(t)$, the moment generating function (MGF) for this system is

$$\mathbb{E}[e^{I_n(t)}] = e(1 - B(t) + B(t)e^s)^n \tag{8}$$

where the factor of e comes from the addition of the primary infection. We have thus characterised the probability distribution for the number of infections $I_n(t)$ arising time t after a bite conferring n hypnozoites, given hypnozoite dormancies are i.i.d. with distribution $B(t)$.

Immunity for a Single Bite

The acquisition of blood-stage immunity is driven by exposure to blood-stage parasites. Continuous and regular exposure is required to maintain high levels of immunity; in the absence of recent exposure, immunity can be lost (Mueller *et al*, 2013). Here, we treat the cumulative number of blood infections experienced by a host as a metric for exposure.

Define $\gamma_n(t)$ to be a random variable describing the gain in antiparasite immunity time t after a single bite conferring n hypnozoites. We propose

$$\gamma_n(t) = \eta e^{-t/b} I_n(t)$$

We assume immunity increases linearly with each primary infection or relapse at a constant rate η. Immunity is also subject to exponential decay at a rate governed by parameter b. As a first approximation, we model immunity for any given mosquito bite to decay from the time of the mosquito bite (or primary infection). A simulated sample path is shown in Figure 3.

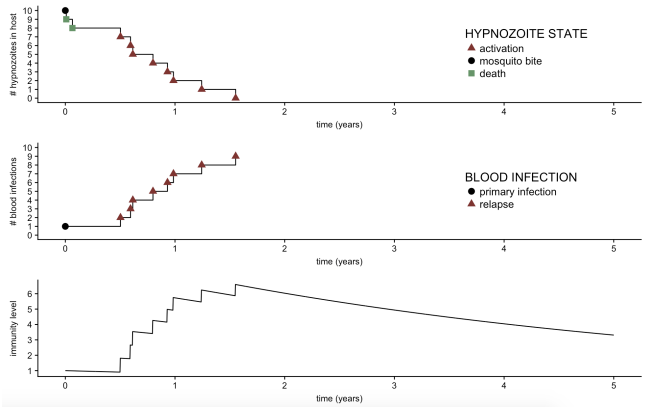

Figure 3: Simulated sample path for a single mosquito bite with $n = 10$ hypnozoites. The top graph tracks the decrease in the hypnozoite reservoir due to death or activation. Two hyonozoites die before activating, but the remaining eight hypnozoites activate to cause relapses, as shown in the middle graph. The bottom graph tracks the immunity $\gamma_{10}(t)/\eta$ gained from infections arising due to the bite. Immunity is boosted with every primary infection or relapse, and decays exponentially at rate $b = 5$ year^{-1} from the time of the mosquito bite. Our model of hypnozoite activation (7) has been simulated using the Gillespie algorithm (Kojima, 2012).

Since $\gamma_n(t)$ is a linear combination of the random variable $I_n(t)$ with MGF (8), we deduce the MGF of $\gamma_n(t)$

$$\mathbb{E}[e^{\gamma_n(t)}] = \exp\left(se^{-t/b}\eta\right)\Big(1 - B(t) + B(t)\exp\left(se^{-t/b}\eta\right)\Big)^n \tag{9}$$

We have now characterised the probability distribution for immunity $\gamma_n(t)$ gained time t after a single bite conferring n hypnozoites, given immunity is boosted linearly at rate η with every primary infection or relapse, and decays exponentially at rate b. We have assumed hypnozoite dormancies are i.i.d. with distribution $B(t)$ given by an underlying within-host model.

Immunity for Fixed n

Let $\{\Phi_n(t), t > 0\}$ be the stochastic process pertaining to the acquisition of immunity from bites conferring exactly n hypnozoites. Recall that bites conferring exactly n hypnozoites follow a Poisson process with rate $g_n\lambda(t)$, where $\lambda(t)$ is the overall bite rate and g_n is the probability of a bite containing n hypnozoites.

We assume that immunity is additive across bites. Let $\tau_1, \tau_2, \tau_3 ...$ denote bite times and $N_n(t)$ denote the number of bites in the interval $[0, t)$; these are governed by a nonhomogeneous Poisson process with rate $g_n\lambda(t)$. The immunity contribution at time t from a mosquito bite with n hypnozoites occuring at time τ_m is described by the random variable $\gamma_n(t - \tau_m)$ with MGF given by equation (9), where we additionally define $\gamma_n(u) = 0 \ \ \forall u < 0$. The overall gain in immunity from bites conferring exactly n hypnozoites $\Phi_n(t)$ time t after birth is therefore given by

$$\Phi_n(t) = \sum_{m=1}^{N_n(t)} \gamma_n(t - \tau_m) \tag{10}$$

We identify (10) as a filtered Poisson, or shot noise process (Parzen, 1999). Figure 4 illustrates a simulated sample path.

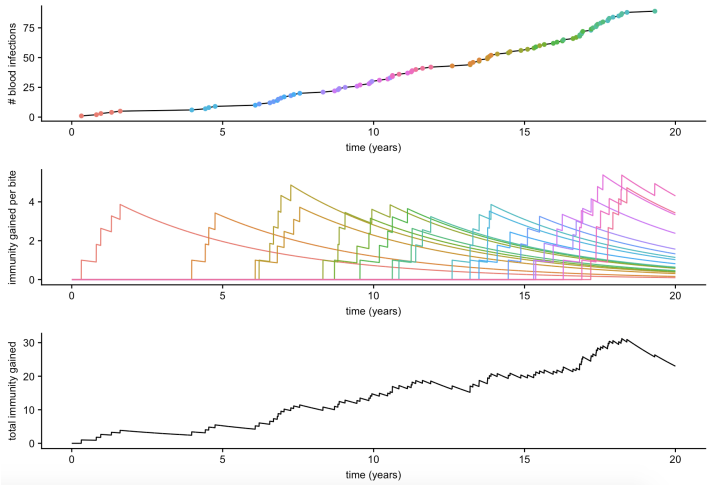

Figure 4: Simulated sample path for immunity and infection arising from bites conferring exactly $n = 10$ hypnozoites, given bites conferring $n = 10$ hypnozoites follow a nonhomogeneous Poisson process of rate $g_{10}\lambda(t) = 0.0025 + 0.0015\sin(2\pi t/365)$ and immunity for each bite decays at rate $b = 5$ year^{-1}. The graph at the top tracks the number of blood infections experienced over time, with each colour representing a different bite. The graph at the middle shows the gain in immunity, described by the random variable γ_{10}/η, for each individual bite; immunity is boosted with each infection, and decays exponentially from the time of the bite. The bottom graph depicts the overall gain in immunity Φ_{10}/η over time from birth, given by the sum of the immunity contributions for individual bites. The underlying model of hypnozoite activation (7) has been simulated using the Gillespie algorithm, while mosquito bites, which follow a nonhomogenous Poisson process, have been simulated using a thinning process (Lewis and Shedler, 1979).

We now derive the MGF for $\Phi_n(t)$, generalising the framework developed by Parzen (1999, pp. 153-155) for a time-inhomogeneous case.

We begin by noting that

$$\mathbb{E}[e^{\Phi_n(t)}] = \sum_{k=0}^{\infty} \mathbb{E}[e^{\Phi_n(t)}|N_n(t) = k] \cdot \Pr[N_n(t) = k]$$

The mean number of bites conferring n hypnozoites in the interval $[0, t)$ is $g_n m(t)$, where g_n is the probability of a bite containing exactly n hypnozoites and $m(t)$ is the mean number of bites in the interval $[0, t)$. Since bites follow a nonhomogenous Poisson process

$$\Pr[N_n(t) = k] = \frac{[g_n m(t)]^k e^{-g_n m(t)}}{k!}$$

Given one arrival in the interval $[0, t)$, the probability of the arrival occurring in the interval $(\tau, \tau + d\tau)$ is

$$\frac{\lambda(\tau)d\tau}{m(t)}$$

Define U to be the random variable with PDF

$$p_u(\tau) = \frac{\lambda(\tau)}{m(t)}, \tau \in [0, t)$$

Then, given k arrivals in the interval $[0, t)$, the conditional distribution of the arrival times $0 < \tau_1 < \tau_2 < ... < \tau_k \leq t$ is equivalent to the distribution of k ordered, independent random variables, each distributed as U. For any real $s_1, ..., s_k$ satisfying $0 \leq s_1 < s_2 < ... < s_k \leq t$, by considering the order statistics $U_{(1)}, ..., U_{(k)}$, we can write the joint distribution

$$f_{\tau_1,...,\tau_k}(s_1, ..., s_k) = k! \prod_{j=1}^{k} p_u(s_j) = \frac{k!}{m(t)^k} \prod_{j=1}^{k} \lambda(s_j)$$

We define

$$\begin{aligned}
\psi(s_1, ..., s_k) &= \mathbb{E}[e^{\Phi_n(t)} | N(t) = k, \tau_1 = s_1, ..., \tau_k = s_k] \\
&= \mathbb{E}\left[\exp\left(\sum_{j=1}^{k} \gamma_n(t - s_j)\right)\right] \\
&= \prod_{j=1}^{k} \mathbb{E}[e^{\gamma_n(t-s_j)}]
\end{aligned}$$

Therefore, we note

$$\begin{aligned}
\mathbb{E}[e^{\Phi_n(t)} | N_n(t) = k] &= \int_0^t ds_1 \int_{s_1}^t ds_2 ... \int_{s_{k-1}}^t ds_k \Phi(s_1, ..., s_k) f_{\tau_1,...,\tau_k}(s_1, ..., s_k) \\
&= \frac{k!}{m(t)^k} \int_0^t ds_1 \lambda(s_1) \int_{s_1}^t \lambda(s_2) ds_2 ... \int_{s_{k-1}}^t \lambda(s_k) ds_k \Phi(s_1, ..., s_k) \\
&= \frac{1}{m(t)^k} \int_0^t ds_1 \lambda(s_1) \int_0^t \lambda(s_2) ds_2 ... \int_0^t \lambda(s_k) ds_k \Phi(s_1, ..., s_k)
\end{aligned}$$

since $\Phi(s_1, ..., s_k)$ is a symmetric function of its arguments.

It follows that

$$\mathbb{E}[e^{\Phi_n(t)} | N_n(t) = k] = \left[\frac{1}{m(t)} \int_0^t \lambda(\tau)\, \mathbb{E}[e^{\gamma_n(t-\tau)}] d\tau\right]^k$$

We can thus determine the MGF for $\Phi_n(t)$ in terms of the MGF for $\gamma_n(t)$

$$\begin{aligned}
\mathbb{E}[e^{\Phi_n(t)}] &= \sum_{k=0}^{\infty} \frac{[g_n m(t)]^k e^{-g_n m(t)}}{k!} \cdot \left[\frac{1}{m(t)} \int_0^t \lambda(\tau)\, \mathbb{E}[e^{\gamma_n(t-\tau)}] d\tau\right]^k \\
&= e^{-g_n m(t)} \sum_{k=0}^{\infty} \frac{1}{k!} \left[g_n \int_0^t \lambda(\tau)\, \mathbb{E}[e^{\gamma_n(t-\tau)}] d\tau\right]^k \\
&= \exp\left\{g_n \int_0^t \lambda(\tau)(-1 + \mathbb{E}[e^{\gamma_n(t-\tau)}]) d\tau\right\}
\end{aligned}$$

Substituting the MGF for $\gamma_n(t)$ (9), we have

$$\mathbb{E}[e^{\Phi_n(t)}] = \exp\Big\{g_n \int_0^t \lambda(\tau)\Big[-1+\exp\left(se^{-(t-\tau)/b}\eta\right)\Big(1-B(t-\tau)+B(t-\tau)\exp\left(se^{-(t-\tau)/b}\eta\right)\Big)^n\Big]d\tau\Big\} \quad (11)$$

Equation (11) provides a description for the probability distribution of $\Phi_n(t)$, the overall gain in immunity from bites conferring exactly n hypnozoites time t after birth. Given a bite rate of $\lambda(t)$ and a probability g_n of a bite containing n hypnozoites, we have modelled model bites conferring n hypnozoites to occur at rate $g_n\lambda(t)$. We have assumed that immunity is additive across bites. For a single bite, we assume immunity is boosted by η for each primary infection or relapse experienced, as well as decaying exponentially at rate b from the time of the mosquito bite. We have taken hypnozoite dormancies to be i.i.d. with distribution $B(t)$

Immunity for Variable n

Let $\{\Phi(t), t>0\}$ be the stochastic process pertaining to the overall acquisition of immunity. Modelling immunity to be additive across bites, the overall gain in immunity $\Phi(t)$ is given by the sum of the immunity contributions $\Phi_n(t)$ for bites conferring exactly n hypnozoites, i.e.

$$\Phi(t) = \sum_{n=0}^{\infty} \Phi_n(t)$$

A simulated sample path is shown in Figure 5.

We now make the assumption that immunity is gained independently for each bite. Then the random variables describing immunity gained cumulatively from bites conferring known numbers of hypnozoites, $\Phi_1(t), \Phi_2(t), \Phi_3(t)...$ can be treated as independent. We compute the MGF for $\Phi(t)$ as a product of the MGFs for $\Phi_n(t)$ (11)

$$\begin{aligned}
\mathbb{E}[e^{\Phi(t)}] &= \prod_{n=0}^{\infty} \mathbb{E}[e^{\Phi_n(t)}] \\
&= \prod_{n=0}^{\infty} \exp\Big\{p_n \int_0^t \lambda(\tau)\Big[-1+\exp\left(se^{-\frac{t-\tau}{b}}\eta\right)\Big(1-B(t-\tau)+B(t-\tau)\exp\left(se^{-\frac{t-\tau}{b}}\eta\right)\Big)^n\Big]d\tau\Big\} \\
&= \exp\Big\{\sum_{n=0}^{\infty} p_n \int_0^t \lambda(\tau)\Big[-1+\exp\left(se^{-\frac{t-\tau}{b}}\eta\right)\Big(1-B(t-\tau)+B(t-\tau)\exp\left(se^{-\frac{t-\tau}{b}}\eta\right)\Big)^n\Big]d\tau\Big\} \\
&= \exp\Big\{\int_0^t \lambda(\tau)\Big[-1+\frac{\exp\left(se^{-\frac{t-\tau}{b}}\eta\right)}{N+1}\sum_{n=0}^{\infty}\Big[\frac{N}{N+1}\Big(1-B(t-\tau)+B(t-\tau)\exp\left(se^{-\frac{t-\tau}{b}}\eta\right)\Big)\Big]^n\Big]d\tau\Big\}
\end{aligned}$$

We note that our MGF is well-defined given

$$\frac{N}{N+1}\Big(1-B(t-\tau)+B(t-\tau)\exp\left(se^{-\frac{t-\tau}{b}}\eta\right)\Big) < 1 \Leftrightarrow B(t-\tau)[\exp\left(se^{-\frac{t-\tau}{b}}\eta\right)-1] < 1/N$$

with $N>0, \eta>0, t-\tau\leq 0, B(t-\tau)\in[0,1]$. If $B(t-\tau)=0$, then our inequality holds. Otherwise, we can equivalently write

$$s < \frac{1}{\eta}e^{\frac{t-\tau}{b}}\log\Big(1+\frac{1}{NB(t-\tau)}\Big)$$

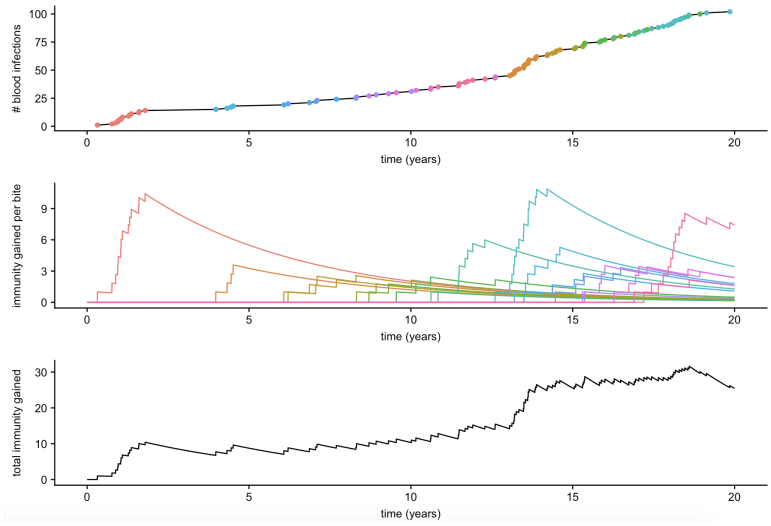

Figure 5: Simulated sample path for immunity and infection in an endemic region with sinusoidal bite rate $\lambda(t) = 0.0025 + 0.0015\sin(2\pi t/365)$. The number of hypnozoites per bite is geometrically distributed with mean $\nu = 10$, and immunity for each bite decays at rate $b = 5$ year^{-1}. The graph at the top tracks the number of blood infections experienced over time, with each colour representing a different bite. The graph at the middle shows the gain in immunity for each individual bite, described by the random variable γ_n/η, where n is the number of hypnozoites conferred by that bite. The bottom graph depicts the overall gain in immunity Φ/η over time from birth, given by the sum of the immunity contributions for individual bites. The underlying model of hypnozoite activation (7) has been simulated using the Gillespie algorithm (Kojima, 2012), while mosquito bites, which constitute a nonhomogenous Poisson process, have been simulated using a thinning process (Lewis and Shedler, 1979).

Noting that $e^{\frac{t-\tau}{b}} \geq 1$ and $\frac{1}{B(t-\tau)} \geq 1$, we deduce

$$\frac{1}{\eta} e^{\frac{t-\tau}{b}} \log\left(1 + \frac{1}{NB(t-\tau)}\right) > \frac{1}{\eta} \log\left(1 + \frac{1}{N}\right)$$

So our MGF is well-defined $\forall t$ given

$$s < \frac{1}{\eta} \log\left(1 + \frac{1}{N}\right)$$

and, in this domain, we have

$$\mathbb{E}[e^{\Phi(t)}] = \exp\left\{ \int_0^t \lambda(\tau) \left[-1 + \frac{\exp\left(se^{-\frac{t-\tau}{b}}\eta\right)}{1 + \nu B(t-\tau)[1 - \exp\left(se^{-\frac{t-\tau}{b}}\eta\right)]} \right] d\tau \right\} \tag{12}$$

Since the MGF for $\Phi(t)$ is well-defined in an open interval around $s = 0$, we can compute the moments of the probability distribution for $\Phi(t)$.

We begin by computing the expectation value of $\Phi(t)$

$$\mathbb{E}[\Phi(t)] = \frac{\partial}{\partial s} \mathbb{E}[e^{\Phi(t)}]\Big|_{s=0} = \eta \int_0^t \lambda(\tau) e^{-\frac{t-\tau}{b}} (1 + \nu B(t-\tau)) d\tau \tag{13}$$

We also determine the variance of $\Phi(t)$

$$\begin{aligned}\text{Var}[\Phi(t)] =& \frac{\partial^2}{\partial s^2}\,\mathbb{E}[e^{\Phi(t)}]\Big|_{s=0} - \Big(\frac{\partial}{\partial s}\,\mathbb{E}[e^{\Phi(t)}]\Big|_{s=0}\Big)^2 \\ =& \eta\int_0^t \lambda(\tau)e^{-\frac{2(t-\tau)}{b}}[\eta + NB(t-\tau)(1+2\eta+2\eta N)]d\tau - \\ & \eta^2\Big[\int_0^t \lambda(\tau)e^{-\frac{t-\tau}{b}}(1+NB(t-\tau))d\tau\Big]^2\end{aligned} \tag{14}$$

We have now characterised the expected value and variance for blood-stage immunity given a time-dependent bite rate $\lambda(t)$. We have modelled the number of hypnozoites conferred per bite to follow a geometric distribution with mean N, and modelled hypnozoite dormancies to be i.i.d. with distribution $B(t)$. We assumed that immunity is gained independently and additively for infections arising from different bites. For a given mosquito bite, immunity is boosted by η for each primary infection or relapse, and decays exponentially at rate b from the time of the bite.

Numerical Results

We have developed a general model of exposure-dependent immunity to vivax malaria. We have assumed immunity is gained independently for different bites, and is, furthermore, additive across bites. Immunity is boosted with each primary infection or relapse, and is also subject to exponential decay over time. By modulating the inoculation rate, we can account for seasonal and environmental changes. We will now examine several cases of biological interest.

Endemic Regions

Consider an individual who remains in an endemic region for a lifetime, and is thus continually at risk of mosquito inoculation. We account for seasonality in inoculation rates, given mosquito transmission is higher in summer than winter in temperate regions, by considering a sinusoidal bite rate, as shown in Figure 6. The graph on the left depicts the seasonally-varying bite rate, while the graph on the right depicts the expected immunity profile of an individual who remains in the region for a lifetime.

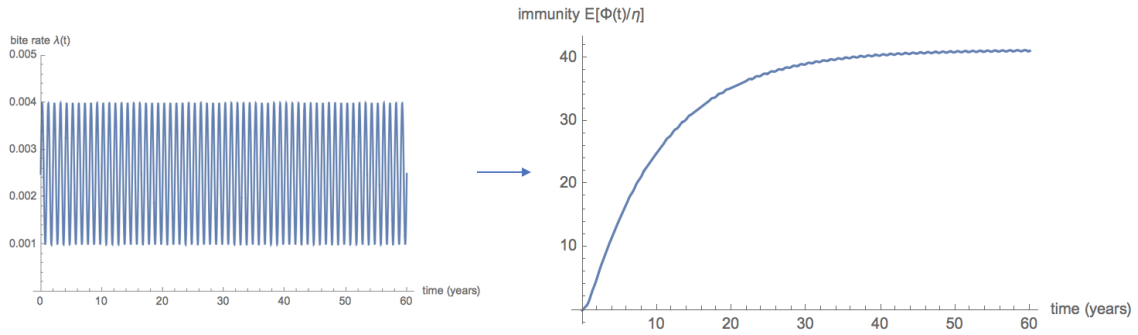

Figure 6: Expected immunity level $\mathbb{E}[\Phi(t)/\eta]$ given a sinusoidal bite rate $\lambda(t) = 0.0025 + 0.0015\sin(2\pi t)$; a mean of $\nu = 10$ hypnozoites per bite and immunity for each bite decaying at rate $b = 10$ year^{-1}.

Our model predicts that immunity is gained rapidly in childhood due to the combined effect of relapses and primary infections. However, there is a kink in the immunity profile in early childhood since there is a period during which only primary infections can occur: although the hypnozoite reservoir can start to be established from birth, there is a delay before relapsing infections can occur. Immunity is expected to stabilise later in adulthood, as the contribution of older bites to overall immunity levels starts to wane significantly.

Travel between Endemic and Non-Endemic Regions

Now consider an individual who spends their adolescence in an endemic region, but who travels to a region with no transmission for a significant period. We compare the immunity profile of a traveller to an individual who remains in an endemic region for a lifetime in Figure 7. The graph on the left shows the infected bite rate for a traveller who temporarily migrates to a non-endemic region for a period of 8.5 years in early adulthood. The graph on the right compares the expected immunity profile the traveller (shown in blue) to the expected immunity profile of an individual who remains in the endemic region (shown in orange), subject to a consistent sinusoidal bite rate over time.

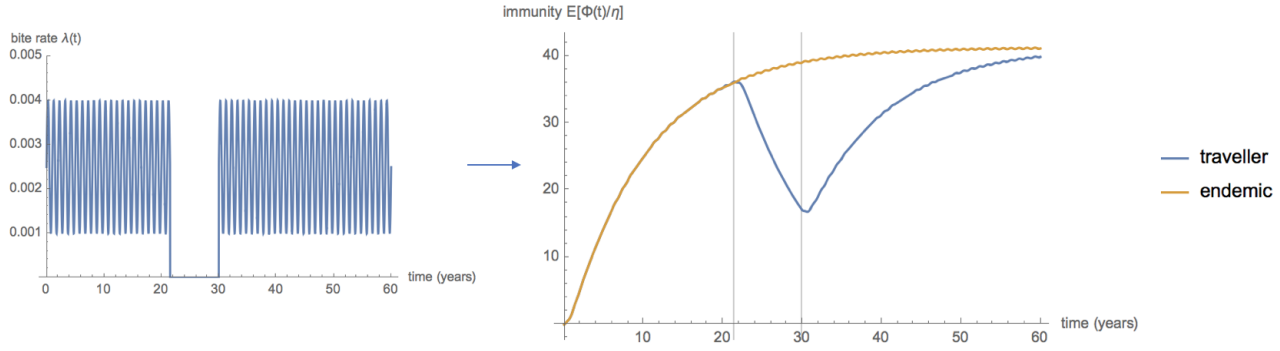

Figure 7: Expected immunity level $\mathbb{E}[\Phi(t)/\eta]$ given a sinusoidal bite rate $\lambda(t) = 0.0025 + 0.0015\sin(2\pi t)$ for $t \in [0, 21.5] \cup [30, 60]$ and zero transmission $\lambda(t) = 0$ for $t \in (21.5, 30)$; a mean of $\nu = 10$ hypnozoites per bite and immunity for each bite decaying at rate $b = 10$ year^{-1}.

Our model predicts that immunity decays significantly in the absence of transmission, after a delay during which immunity is still gained from relapses arising from the activation of previously-established hypnozoites. Immunity is re-gained rapidly upon return to the endemic region.

Declining Transmission

Consider an endemic region subject to declining levels of mosquito transmission, as a result of control efforts. We consider the immunity profile of an individual in such a region over a lifetime in Figure 8. The graph on the left depicts the declining bite rate, subject to seasonality, while the graph on the right depicts the expected immunity profile of an individual subject to the declining bite.

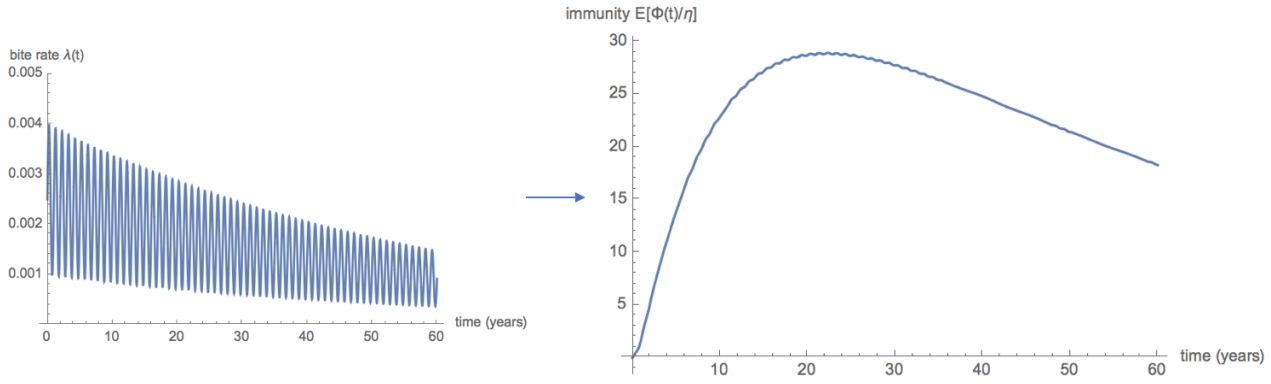

Figure 8: Expected immunity level $\mathbb{E}[\Phi(t)/\eta]$ given a sinusoidal bite rate, subject to exponential decay over time $\lambda(t) = [0.0025 + 0.0015\sin(2\pi t)]\exp(-t/60)$; a mean of $\nu = 10$ hypnozoites per bite and immunity for each bite decaying at rate $b = 10$ year^{-1}.

Our model predicts that declining transmission levels can lead to a decrease in immunity over time since recent infections contribute more strongly to immunity that previous infections. While the prevalence of infection may decrease with declining transmission, the severity of infection may concomitantly increase after a point.

Vaccine Rebound Effect

We will now examine the vaccine rebound effect through our model. A clinical trial of the malaria vaccine RTS,S/AS01 exhibited this dynamic (Olotu, 2016). The vaccine, which targeted sporozoites (pre-erythrocytic stages) and thus prevented the development of blood infection, initially reduced the risk of clinical malaria (Olotu, 2016). However, the efficacy of the vaccine was found to wane over time. In later years, vaccinated children were found to be more susceptible to clinical infection than unvaccinated children (Olotu, 2016).

We model the efficacy of such a vaccine as a decrease in the probability $p_{\text{success}}(t)$ of an infected mosquito bite being successful i.e. leading to a primary blood infection and the establishment of hypnozoites. We assume that all infected mosquito bites for unvaccinated individuals are successful. We assume the vaccine initially prevents blood infection i.e. $p_{\text{success}}(0) = 0$, but that vaccine efficiency wanes over time, as shown in Figure 9. The bite rate, which corresponds only to successful bites, is different for vaccinated individuals and unvaccinated individuals in the same endemic region. If an unvaccinated individual is subject to (successful) bite rate $\lambda(t)$, then a vaccinated individual is subject to (successful) bite rate $p_{\text{success}}(t)\lambda(t)$, where $p_{\text{success}}(t)$ describes the probability of a bite being successful time t after vaccination.

Figure 10 compares the immunity profiles for vaccinated and unvaccinated individuals in the same endemic region. Successful bite rates and expected immunity profiles for vaccinated and unvaccinated individuals are shown in blue and orange respectively.

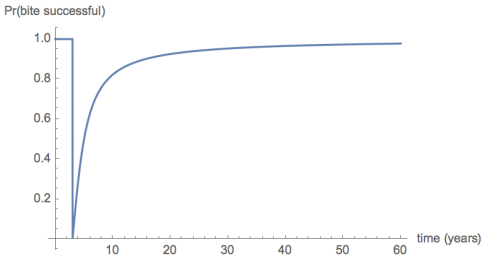

Figure 9: Probability of an infected mosquito bite being successful for an individual vaccinated at age 3, modelled to be $p_{\text{success}}(t) = 2/\pi \arctan\left((t-3)/2\right)$

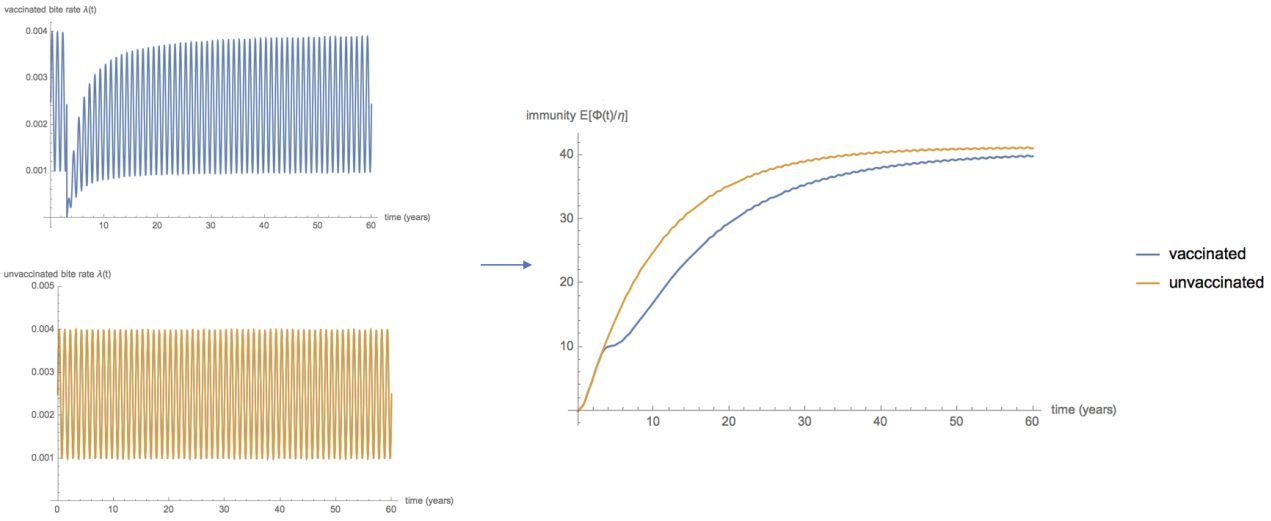

Figure 10: Expected immunity level $\mathbb{E}[\Phi(t)/\eta]$ for vaccinated and unvaccinated given a sinusoidal infected bite rate $\lambda(t) = 0.0025 + 0.0015\sin(2\pi t)$; a mean of $\nu = 10$ hypnozoites per bite and immunity for each bite decaying at rate $b = 10$ year^{-1}. The successful bite rate for vaccinated individuals becomes $p_{\text{success}}(t)\lambda(t)$.

Our model predicts that a vaccine targeting pre-erythrocytic stages with waning efficacy delays the natural acquisition of blood-stage immunity by reducing exposure to blood-stage parasites. We have thus qualitatively captured the vaccine rebound effect. If this delay is of sufficient magnitude, it may adversely impact clinical outcomes. By coupling our blood-stage model of immunity with more sophisticated vaccine models, we may be able to glean insights relevant to vaccine development.

Discussion

We have developed a stochastic within-host model of exposure-dependent blood-stage immunity to *Plasmodium vivax*. We have sought to capture two complementary dynamics driving immunity levels: the boosting of immunity with cumulative exposure, and the decay of immunity over time. Previous models examining blood-stage immunity to *Plasmodium vivax* have examined interactions between human and parasite cells (see, for example, McQueen and McKenzie, 2008; Kerlin and Gatton, 2015). Here, we have considered the acquisition

of blood-stage immunity to *Plasmodium vivax* given an arbitrary risk of exposure. I am unaware of an existing within-host model for *Plasmodium vivax* that addresses this problem.

We have extended the work of White *et al* (2014), embedding a model of hypnozoite activation in a framework mimicking mosquito inoculation. We have proposed a novel way of conceptualising immunity gained through successive infections as a filtered Poisson process. We can adapt our model to reflect a broad range of transmission settings and biological phenomena. Having derived a moment-generating function to describe blood-stage immunity, we can readily extract parameters of epidemiological significance in biologically-relevant scenarios. Although clinical trials and longitudinal studies are central to our understanding of immunity in transmission settings, they are subject to significant logistic and economical constraints. A mathematical model of blood-stage immunity like ours can provide key epidemiological insights.

Our model, however, exclusively the effects of exposure on immunity. We have neglected to incorporate more biologically complex facets of immunity in our model. There are clinical data to suggest that age-related, physiological factors may play a role in immunity, independent of exposure (Rodriguez-Barraquer, 2018). Children, for instance, still have maturing immune systems. Further evidence suggests that immunity to vivax malaria is strain-specific, with an indeterminate degree of cross-protection (Mueller *et al*, 2013). Nonlinear relationships may exist between levels of immunity to *Plasmodium vivax* and transmission intensities, due to variations in the diversity levels the *Plasmodium vivax* parasite populations. The inclusion of such dynamics on our mathematical model may allow deeper insights to be drawn into the acquisition of immunity to *Plasmodium vivax*.

References

World Health Organization, 2017. World Malaria Report 2017. World Health Organisation.

Naing, C., Whittaker, M.A., Wai, V.N. and Mak, J.W., 2014. Is Plasmodium vivax malaria a severe malaria: a systematic review and meta-analysis. *PLoS neglected tropical diseases*, 8(8), p.e3071.

Howes, R.E., Battle, K.E., Mendis, K.N., Smith, D.L., Cibulskis, R.E., Baird, J.K. and Hay, S.I., 2016. Global epidemiology of Plasmodium vivax. *The American journal of tropical medicine and hygiene*, 95(6_Suppl), pp.15-34.

Mueller, I., Galinski, M.R., Tsuboi, T., Arevalo-Herrera, M., Collins, W.E. and King, C.L., 2013. Natural acquisition of immunity to Plasmodium vivax: epidemiological observations and potential targets. In *Advances in parasitology* (Vol. 81, pp. 77-131). Academic Press.

McQueen, P.G. and McKenzie, F.E., 2008. Host control of malaria infections: constraints on immune and erythropoeitic response kinetics. *PLoS computational biology*, 4(8), p.e1000149.

Kerlin, D.H. and Gatton, M.L., 2015. A simulation model of the within-host dynamics of Plasmodium vivax infection. *Malaria journal*, 14(1), p.51.

De Zoysa, A.P., Mendis, C., Gamage-Mendis, A.C., Weerasinghe, S., Herath, P.R. and Mendis, K.N., 1991. A mathematical model for Plasmodium vivax malaria transmission: estimation of the impact of transmission-blocking immunity in an endemic area. *Bulletin of the World Health Organization*, 69(6), p.725.

White, M.T., Karl, S., Battle, K.E., Hay, S.I., Mueller, I. and Ghani, A.C., 2014. Modelling the contribution of the hypnozoite reservoir to Plasmodium vivax transmission. *Elife*, 3, p.e04692.

White, N.J. and Imwong, M., 2012. Relapse. In *Advances in parasitology* (Vol. 80, pp. 113-150). Academic Press.

Eick, S.G., Massey, W.A. and Whitt, W., 1993. The physics of the Mt/G/inf queue. *Operations Research*, 41(4), pp.731-742.

Holman, D.F., Chaudhry, M.L. and Kashyap, B.R.K., 1983. On the service system MX/G/inf. European Journal of Operational Research, 13(2), pp.142-145.

Kojima, F., 2012. Simulation algorithms for continuous time Markov chain models. *Simulation and Modeling Related to Computational Science and Robotics Technology: Proceedings of SiMCRT*, 37(3).

Lewis, P.W. and Shedler, G.S., 1979. Simulation of nonhomogeneous Poisson processes by thinning. *Naval research logistics quarterly*, 26(3), pp.403-413.

Parzen, E., 1999. *Stochastic processes* (Vol. 24). SIAM.

Olotu, A., Fegan, G., Wambua, J., Nyangweso, G., Leach, A., Lievens, M., Kaslow, D.C., Njuguna, P., Marsh, K. and Bejon, P., 2016. Seven-year efficacy of RTS, S/AS01 malaria vaccine among young African children. *New England Journal of Medicine*, 374(26), pp.2519-2529.

Rodriguez-Barraquer, I., Arinaitwe, E., Jagannathan, P., Kamya, M.R., Rosenthal, P.J., Rek, J., Dorsey, G., Nankabirwa, J., Staedke, S.G., Kilama, M. and Drakeley, C., 2018. Quantification of anti-parasite and anti-disease immunity to malaria as a function of age and exposure. *Elife*, 7, p.e35832.